npj | aging

Article

Published in partnership with the Japanese Society of Anti-Aging Medicine

https://doi.org/10.1038/s41514-025-00253-w

Nothobranchius furzeri: a vertebrate model for studying cardiac aging and cellular senescence

Xueling Ma[1,2,5], Yonghe Ding[1,4,5], David Mondaca-Ruff[1], Xinyue Zhang[2], Yu Lu[3], Baul Yoon[1], Feixiang Yan[1], Yanyan Liang[1], Maryam Moossavi[1] & Xiaolei Xu[1] ✉

African turquoise killifish (*Nothobranchius furzeri*) is the shortest-lived vertebrate that can be bred in captivity, making it an ideal model organism for aging studies. However, whether the animal can be used for studying cardiac aging and whether cellular senescence contribute to this ageing process remain unclear. Here, we conducted a longitudinal study on the GRZ strain, aiming to identify phenotypic and functional markers for cardiac aging. We found that cardiac ageing in GRZ fish can be measured by comparing fish at 16 weeks to 8 weeks of age, using systemic markers such as body/fin coloration, body weight, BMI, cardiac ageing markers such as EF, E/A ratio, and swimming capacity, and cellular senescence markers such as SA-β-gal staining, p15/p16, γ-H2A.X, and SASP markers. Senolytic treatment with D (Dasatinib) and Q (Quercetin) from 12 to 16 weeks mitigated senescence and decelerated cardiac ageing. Together, our findings established GRZ as a useful vertebrate model for studying cardiac ageing and related cardiac senescence.

Aging is a complex biological process characterized by a progressive decline in physiological functions, resulting in gradual deterioration of organ systems and increased susceptibility to diseases[1,2]. Among these systems, the cardiovascular system is particularly affected. Cardiac aging involves structural and functional changes in the heart over time, contributing to a higher risk of cardiovascular disease in the elderly. To study cardiac aging, it is crucial to identify phenotypic and functional traits that can be used to quantify the cardiac aging process, enabling reliable differentiation of biological age from chronological age, prediction of cardiac aging trajectories, and assessment the effectiveness of gerotherapeutic strategies. In support of this goal, international initiatives such as the Aging Biomarker Consortium (ABC) have been established to coordinate biomarker discovery and validation efforts[3,4]. Decline of echocardiographic measurements of left ventricular function such as ejection fraction and E/A ratio are well-documented clinical indicators for cardiac diseases, which have been also associated with cardiac aging[5,6]. In humans, exercise capacity via treadmill assay has been used as an important index for assessing both cardiac diseases and cardiac aging[7]. More clinical and molecular features of cardiovascular aging has been recently reviewed[8]. Some biomarkers of aging are not only indicators but also active drivers of the aging process, which are termed as the "hallmarks of aging"[9] Among the twelve hallmarks of systemic aging, eight are proposed to play critical roles in cardiac aging, including dysregulated autophagy, loss of proteostasis, genomic instability, epigenetic alterations, mitochondrial dysfunction, cell senescence, dysregulated neurohormonal signaling, and inflammation[10].

Cellular senescence is one of the twelve known hallmarks of aging, referring to a process in which cell permanently stop dividing in response to stress or damage, accumulating within the body over time[9]. These senescent cells subsequentially secret "senescence-associated secretory phenotype" (SASP) factors that promote inflammation and accelerate the aging process of the neighboring cells. The accumulation of senescent cells in the heart could potentially lead to impaired contractility and reduced vascular function, contributing to age-related cardiovascular decline[11]. Examining expression levels of cell cycle arrest markers such as *p21, p27* and SASP markers such as *il-6, il-8, il-10* and *tnf-alpha* was used to evaluate cellular senescence[12,13].

The African turquoise killifish (ATK, *Nothobranchius furzeri*) is emerging as a unique vertebrate model in aging research due to its exceptionally short lifespan and the conservation of aging-related biomarkers across vertebrates[14,15]. The GRZ strain caught the most attention, because this is an ATK line with the shortest lifespan that can be completed within 4 ~ 6 months[16]. While increased SA-ß-gal staining, oxidative stress, and

[1]Department of Biochemistry and Molecular Biology, Department of Cardiovascular Medicine, Mayo Clinic, Rochester, MN, USA. [2]School of Nursing, Beijing University of Chinese Medicine, Beijing, China. [3]Institute of Traditional Chinese Medicine Information, China Academy of Traditional Chinese Medicine, Beijing, China. [4]Present address: The Affiliated Hospital of Qingdao University & Biomedical Sciences Institute, Qingdao Medical College of Qingdao University, Qingdao, 266021, China. [5]These authors contributed equally: Xueling Ma, Yonghe Ding. ✉e-mail: xu.xiaolei@mayo.edu

reduced regenerative capacity have been reported in the aged hearts of this animal model[17–20], the baseline process of cardiac aging has not been defined. Thus, in this study, we aim to fill this knowledge gap by carrying longitudinal studies of the GRZ strain, aiming to identify markers that can reliably quantify cardiac aging, particularly non-invasive assays that can be conducted in living animals. Additionally, we investigated whether cellular senescence contribute to cardiac aging in this fish model and whether eliminating senescent cells exerts gerotherapeutic effects.

Results

Body color, body weight and BMI indices in GRZ killifish during physiological aging

Prompted by the observation that the body color of aged killifish appears less vivid than young fish (Fig. 1a), we developed a platform to quantify body color in this animal. Compared to fish at 8 weeks of age, the body coloration of both male and female fish declined significantly when they reach 16 weeks old (Fig. 1b, c), with the changes in females milder than in males. The color differences in male fish can be more easily detected in their fins, as indicated by quantification of the yellow hues in their tail fins (Fig. 1d, f) or the coloration of their anal fins (Fig. 1e, g).

In male fish, their body weight initially increases from 8 weeks to 16 weeks of age, but then reduces at 20 weeks of age (Fig. 2a). Similar findings were noted in female fish, but the reduction at 20 weeks of age was not statistically significant (Fig. 2b). These changes are more difficult to detect by using body length as a phenotyping trait (Fig. 2c, d), as indicated by nearly undetectable changes of body length in females. By contrast, these two-phased changes of body size can be more sensitively detected by using BMI as a phenotyping index (Fig. 2e, f).

Together, these results suggest that BMI is probably the most sensitive phenotypic trait that can be used to quantify changes of body size along the aging process, which is followed by body weight. In addition, coloration could serve as a useful visual marker of aging in male killifish.

EF, E/A ratio, and swimming capacity changes in GRZ killifish during physiological aging

A killifish heart appears similar to a zebrafish heart (Fig. S2). To directly quantify physiological cardiac aging, we first carried out echocardiography studies. Compared to 8 weeks of age, ejection fraction (EF%) declined significantly at 16 weeks of age in both males and females (Fig. 3a, b, for representative Echo movies, see Supplemental Video). Reduced EF can be noted in males, but not in females at 12 weeks of age. Despite a trend of EF reduction at 16 weeks of age, no significant declines in EF were detected at 20 weeks of age compared to 16 weeks old in both male and female. Next, we performed Doppler echocardiography and revealed a significant increase in the E/A ratio between 8 weeks vs 16 weeks of age in both male and female. No significant changes in E/A ratio were noted between 16 weeks and 20 weeks of age (Fig. 3c, d).

The highest swimming capacity was noted in killifish at 8 weeks of age in both male and female, which was then declined at 16 weeks of age. Like EF %, this decline was noted in males starting at 12 weeks of age, but not in females. No further decline of swimming capacity was noted from 16 weeks to 20 weeks of age in both sexes (Fig. 3e, f).

Cellular senescence increases during cardiac aging in GRZ killifish

To determine whether and when cellular senescence occurs during physiological cardiac aging in the killifish, we first stained sectioned hearts to evaluate the senescence-associated beta-galactosidase (SA-β-gal) activity, a well-recognized biomarker for cellular senescence. We detected significantly increased SA-β-gal activity from 8 weeks to 16 weeks of age, while it appears to be further increased but not statistically significant at 20 weeks of age compared to 16 weeks (Fig. 4a, b). Next, we carried out immunofluorescence staining experiments to examine expression of p15/p16, another cellular senescence marker, and γ-H2A.X, a DNA damage marker. Significantly increased γ-H2A.X and p15/p16 staining signals were detected at 16 weeks of age (Fig. 4c–f), mainly in non-cardiomyocytes rather than cardiomyocytes, as indicated by the poor overlap between γ-H2AX signal and the sarcomeric marker α-Actinin; as well as between the p15/p16 staining and the cardiomyocyte nuclear marker Mef2. Future studies are warranted to co-stain these senescence markers with markers for other cardiac cell types such as fibroblast, endocardial cells and epicardial cells, which could uncover novel functions of cellular senescence in cardiac aging.

To seek additional evidence for cellular senescence, we conducted quantitative RT-PCR analysis to determine the expression levels of cell cycle and senescence-associated secretory phenotype (SASP) related markers. We noted significantly upregulated expression of *p21, il-6, il-8* and *tnf-α* at 16 weeks old (Fig. 5a–f). Together, these data support the statement that increased cellular senescence occurs in the heart of African turquoise killifish. Besides accumulated oxidative stress[21], cellular senescence could also contribute to its cardiac aging process.

Senolytic drug treatment with Dasatinib and Quercetin (D + Q) is effective in decelerating cardiac aging in GRZ killifish

To determine the role of cellular senescence on physiological cardiac aging in killifish, we assessed the effects of D + Q, a well-established senolytic drug combination to selectively eliminate senescent cells[21]. 0.5 mg/kg D and 5 mg/kg Q was administered by oral gavage to male killifish every other day from 12 weeks to 16 weeks of age that were housed individually in single tanks. Non-invasive cardiac function and swimming endurance assays were carried out at 16 weeks and 20 weeks of age, while invasive assays such as SA-β-gal staining, immunofluorescence staining and qRT-PCR were performed at 20 weeks of age (Fig. 6a). While D + Q treatment didn't have any significant impact on BMI or body weight (Fig. 6b, c), significantly decelerated cardiac aging, as indicated by more vivid body color, partially rescued EF%, and restored swimming capacity were detected in treated vs untreated control group at 16 weeks (Fig. 6d–g). The effectiveness of D + Q treatment in attenuating cellular senescence was further supported by the detection of significantly decreased SA-β-gal activity, reduced expression of cellular senescence marker of p15/p16 and DNA damage marker of γ-H2AX (Fig. 7a–f), and significant downregulation of SASP transcripts, including *p21, tnf-α and il-6* (Fig. 7g–i) in the D + Q treated group at 20 weeks of age.

Discussion

The primary motivation for establishing the killifish GRZ strain as an animal model for studying cardiac aging is its short lifespan. Compared to human, mice and zebrafish with average lifespans of approximately 80 years, 3 years, and 4 years, respectively, the GRZ strain has an average lifespan of only 4–6 months. Here, we carried longitudinal studies of GRZ and defined baseline process of cardiac aging. We identified a panel of markers that can be used to quantify systemic aging, cardiac aging or cellular senescence in GRZ at 16 weeks of age comparing to fish at 8 weeks of age (Fig. 8).

Our study demonstrates that body color, particularly in male tail fins and anal fins, can be a convenient visual phenotypic marker for physiological aging in the African turquoise killifish. During aging process in humans, the number of melanocytes is thought to decrease by ~10–20% per decade, giving rise to the pale skin or patches of hypo-pigmentation associated with chronologically aged skin[22,23]. This loss of pigmentation corelates with other physiological declines during the aging process, including reduced heart function, decreased cardiac contractility, and increased fibrosis[24]. Similar correlations have been reported in animal models, such as rodents and zebrafish[25]. However, cautions must be exerted when using body color as a biomarker for ageing, especially in relation to cardiac function, because color loss can also be triggered by stress, disease, or even poor housing. It remains to be determined whether the fading down of body color is a direct consequence of poor circulation resulting from cardiac dysfunction or a metabolic activity that reflects systemic health.

In both human and animal models, BMI and weight are commonly used as indicators of overall health, reflecting a balance between muscle mass, fat distribution, and organ function. In humans, BMI and body weight are frequently associated with aging-related cardiac dysfunction, with a

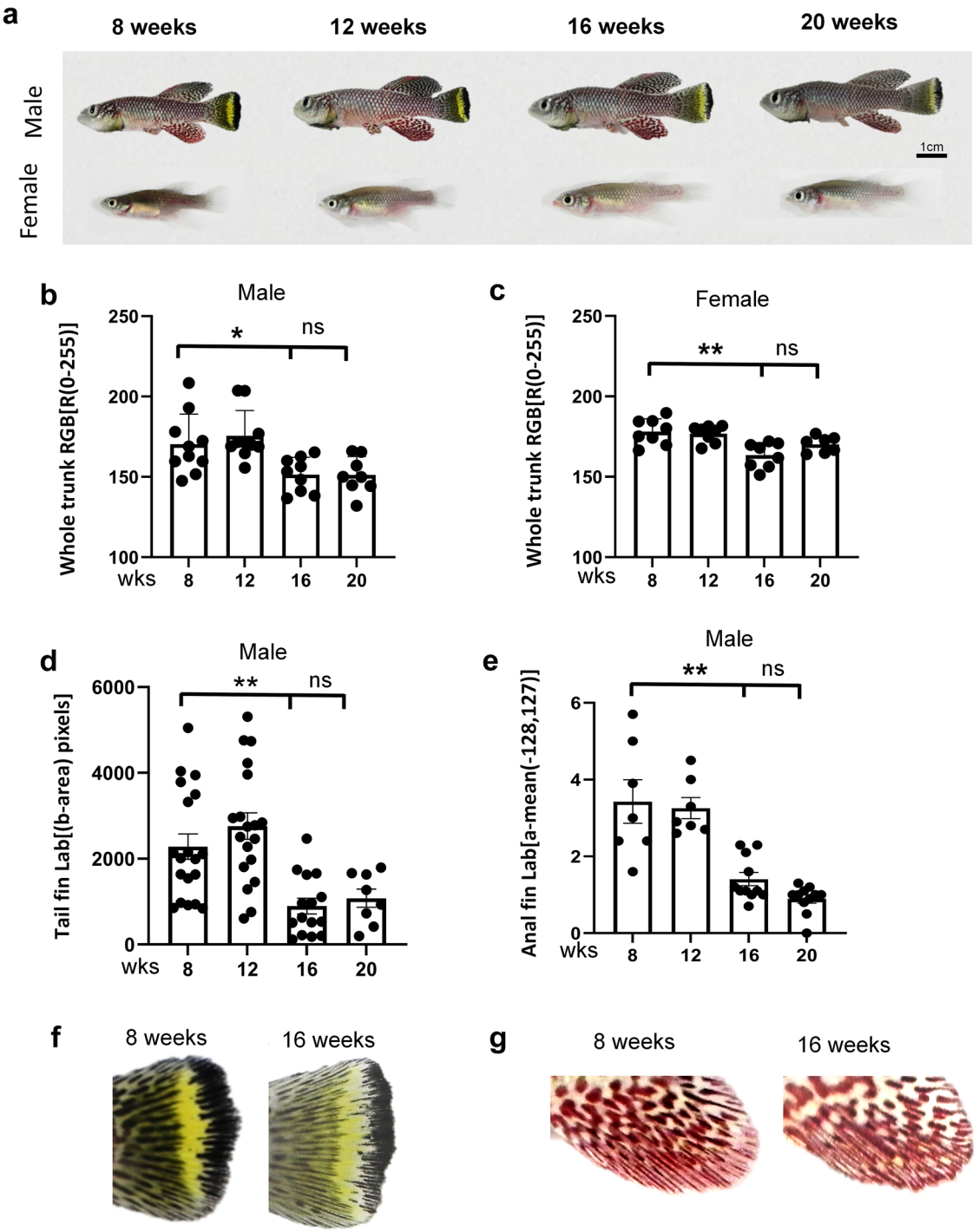

Fig. 1 | Characterization of body color changes in the GRZ killifish during physiological aging. a Representative images of young and aged male and female African turquoise killifish showing surface color changes during aging. Scale bar 1 cm. **b**, **c** Quantification of body coloration in 8-week-old and 16-week-old killifish. **b** Whole trunk RGB[R(0-255)] of male; **c** whole trunk RGB[R(0-255)] of Female; **d** Analysis of tail fin coloration in male killifish. Y-axis: Tail fin Lab[(b-area) pixels]. **e** Quantification of anal fin coloration in male killifish. Y-axis: Anal fin Lab [a-mean (−128,127)]. **f, g** Representative images of tail fin and anal fin. RGB and LAB color values were used for precise color analysis. Images were captured under standardized conditions to ensure consistency and minimize background interference. $n = 7–9$, One-way ANOVA, Tukey post hoc, $^{*}p < 0.05$, $^{**}p < 0.01$.

gradual loss of lean body mass and an increase in body fat often corelating with deteriorating cardiovascular health[26]. Incident heart failure (HF) in older adults is associated with a disproportionate loss of lean mass, particularly among men. The prognostic implications are significant, with key sex-specific effects on physical function, frailty, disability, and pharmacodynamics[27,28]. Similarly, in rodents, aging results in both a reduction in body weight and a decline in cardiac performance, underscoring the interdependence of these factors in the aging process[29]. In zebrafish, reduction in growth rate, body weight, and BMI are also associated with the onset of cardiac dysfunction[30]. In the GRZ strain with a short lifespan, BMI and body weight undergo constant changes along the aging process, which can be broadly divided into two phases: a growth phase that peaks at 16 weeks of age, followed by a shrinking phase where both indices decrease after 16 weeks of age. Interestingly, during the early phase of the

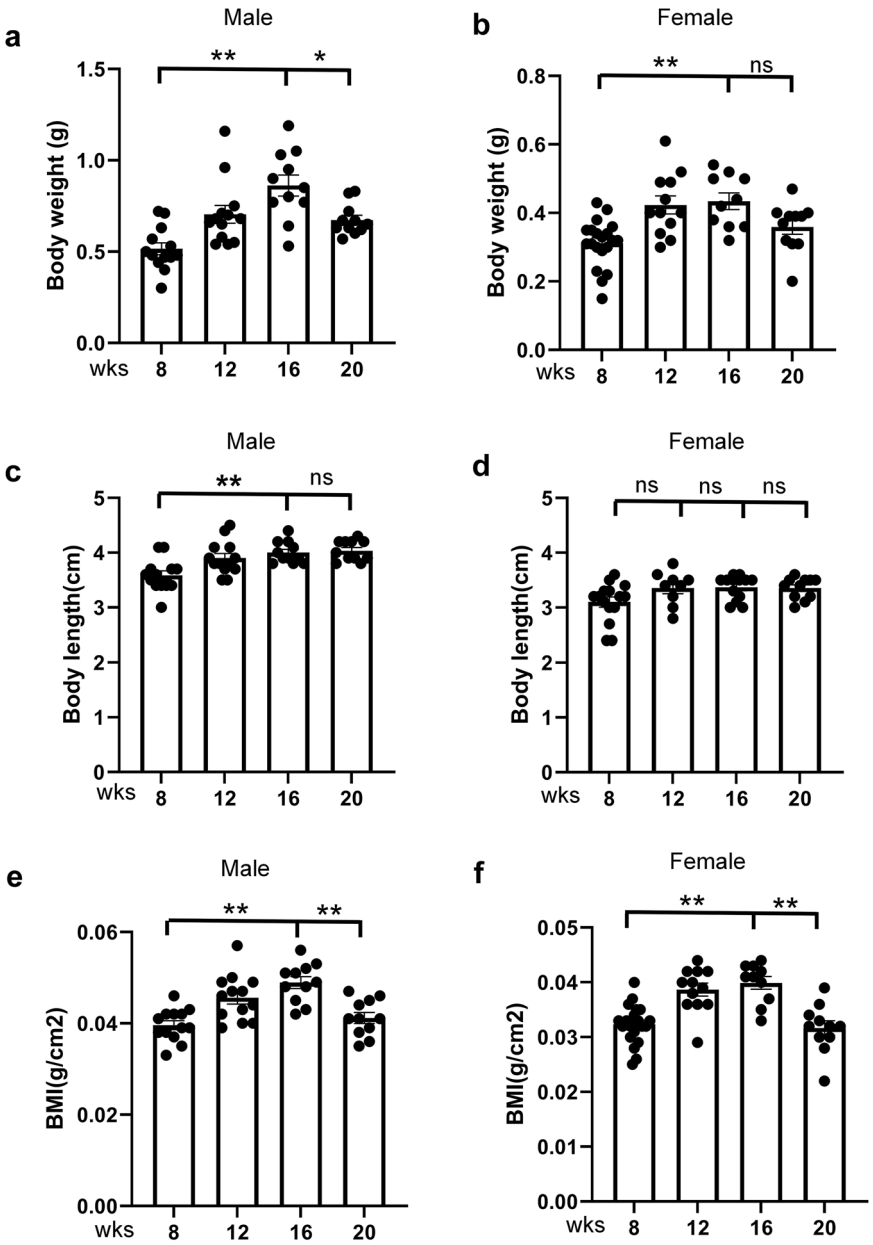

Fig. 2 | Changes in body weight, BMI, and body length in the GRZ killifish during physiological aging. a, **b** Body weight measurement in both male and female killifish from 8 to 20 weeks of age. **c, d** Body length quantification in male killifish from 8 to 20 weeks of age. **e, f** BMI calculation from 8 to 20 weeks of age. $n = 10–13$, One-way ANOVA, Tukey post hoc, $^{*}p < 0.05$, $^{**}p < 0.01$.

process before 16 weeks, an ageing GRZ heart manifests a unique feature-reduced cardiac functions accompanied by increased body size. The transition from growth to shrinkage at 16 weeks of age likely reflects complex metabolic and physiological mechanisms, which warrants further investigation. Comparing to body weight, BMI demonstrated greater sensitivity as a phenotyping index for quantifying the aging process, whereas body length is the least useful index, as it barely changes with aging. Thus, we recommend BMI over body weight as a phenotypic marker when measuring physiological aging. Of note, a direct correlation between BMI and heart function has yet to be established by our present data. Future studies of BMI in lean vs. obese fish at different ages are warranted, which would deepen our understanding of the relationship between BMI and cardiac aging.

Cardiac aging in killifish is characterized by a decline in the ejection fraction (EF) by 16 weeks of age, with males showing an earlier decline at 12 weeks of age. The E/A ratio, which reflects diastolic function, also exhibited changes. These changes resemble those observed in other species, including humans, where males tend to experience earlier cardiac function decline. Both parameters have been previously used to determine the biological age of the heart in mice and to assess the effectiveness of anti-aging therapies such as treatment with D + Q[31].

In humans, reduced physical performance, particularly in aerobic capacity, is often linked to age-related cardiac deterioration, probably owing to diminished cardiac output, reduced oxygen delivery to tissues, and increased vascular resistance[32–34]. This decline in physical endurance is evident in tasks such as walking or climbing stairs and serves as an early indicator of heart failure[35]. Similarly in aging rodents, decreased physical performance has been linked to reduced cardiac function and compromised metabolic health[36]. In zebrafish, swimming tests have been widely used to assess physical fitness, with declines in swimming endurance linked to age-related cardiovascular decline[37]. In the present study, we found that swimming endurance is peaked at 8 weeks of age in the GRZ strain, starts to decline at 12 weeks of age, significantly declines by 16 weeks of age, and continues to decrease at 20 weeks of age. Treatment with D + Q rescued the reduced swimming endurance. Together, these data indicated that swimming endurance can serve as a useful functional marker for quantifying cardiac aging in killifish.

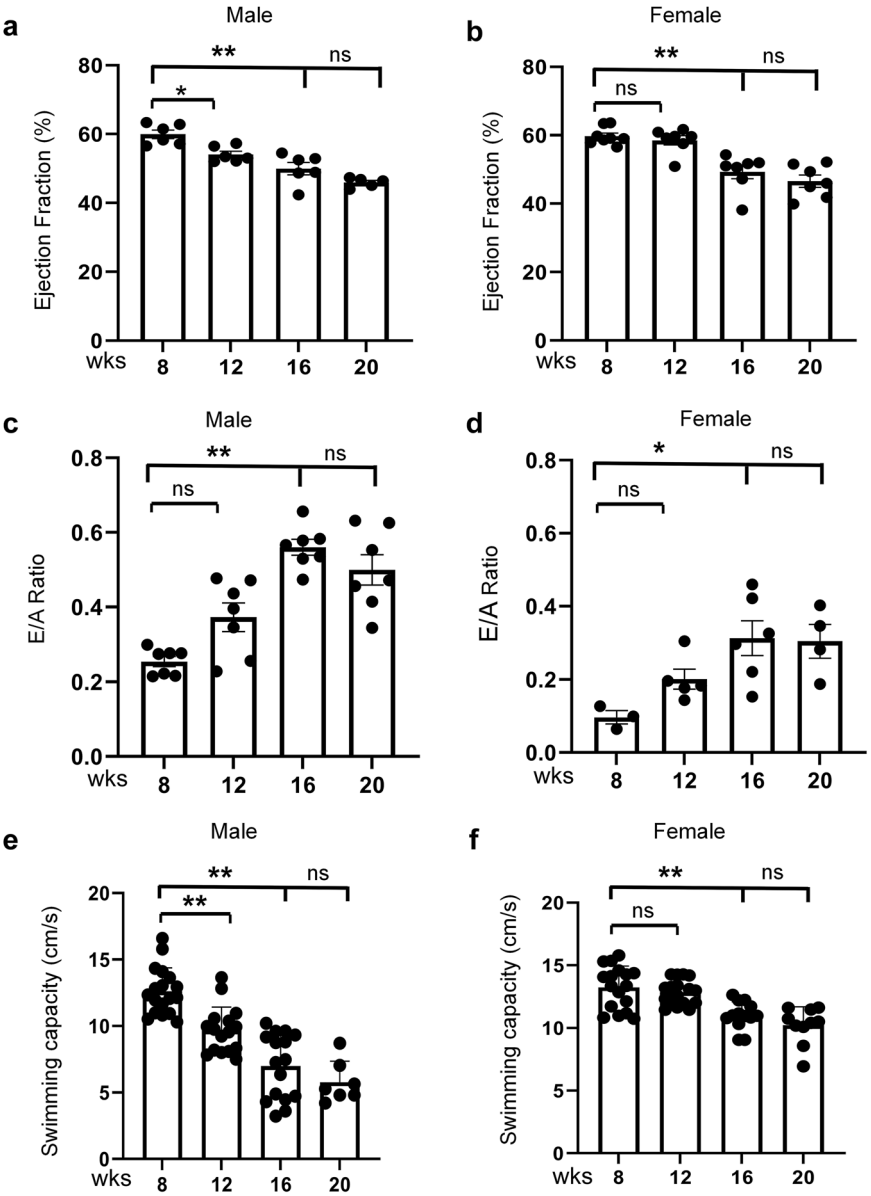

Fig. 3 | Characterization of cardiac function and swimming capacity in the GRZ killifish during physiological aging. a, b Ejection fraction (EF%) in male and female killifish from 8 to 20 weeks of age. **c, d** E/A ratio measured by Doppler echocardiography in killifish from 16 to 20 weeks of age. **e, f** Swimming capacity, assessed by endurance tests from 16 to 20 weeks of age. $n = 4–17$. One-way ANOVA, Tukey post hoc, $^{*}p < 0.05$, $^{**}p < 0.01$.

At the cellular level, we observed increased SA-β-gal activity and upregulation of senescence markers such as p15/p16, γ-H2AX, and inflammatory cytokines like IL-6 and TNF-α in the hearts of aged killifish. These molecular changes mirror findings in mammalian models and suggest that cellular senescence plays a crucial role in cardiac aging. The accumulation of senescent cells leads to impaired tissue repair and a pro-inflammatory environment, accelerating functional decline in the heart. Having demonstrated that cellular senescence did occur during physiological cardiac aging in the killifish GRZ strain, we went on to test the well-known senolytic drug combination D + Q. Indeed, treatment with this drug combination slowed the aging process, reduced senescence markers, and improved cardiac function in the killifish model. Interestingly, certain aging indices at 16 weeks, such as body color and swimming capacity, seems be rescued to a level that is even better than untreated fish at 12 weeks (Fig. 6d–f). This data underscored strong contribution of cellular senescence to cardiac aging, which might already negatively affect fish at 12 weeks of age. While this observation needs to be further validated and explored in the future, our findings confirmed that cellular senescence plays a conserved and significant role in cardiac aging, supporting the use of GRZ as a sensitive vertebrate model for investigating cardiac cellular senescence.

The present study has several limitations. First, while we compare cardiac markers between 8 weeks and 16 weeks of age, this period represents an early phase when BMI and body weight are still increasing. This unique phenomenon does not occur in other animal models with longer lifespans. Second, the present study did not examine the later phase of cardiac aging that occurs after 16 or even 20 weeks of age, when BMI and body weight begin to decrease. This later phase is interesting because it corresponds to the most senior years in humans, e.g. post 65–75 years of age. This phase is more challenging to study because <20% fish survive to this stage, which necessitates a significantly larger initial animal population for meaningful data analysis. Third, baseline measurements must be interpreted in the context of housing and feeding conditions specific to our fish facility. It is well known that differences in fish density and feeding regimens can significantly impact the aging process[38].

Despite these challenges, we believe that the African turquoise killifish presents a unique model organism for cardiac aging research, offering unprecedented opportunities for both pharmacological and

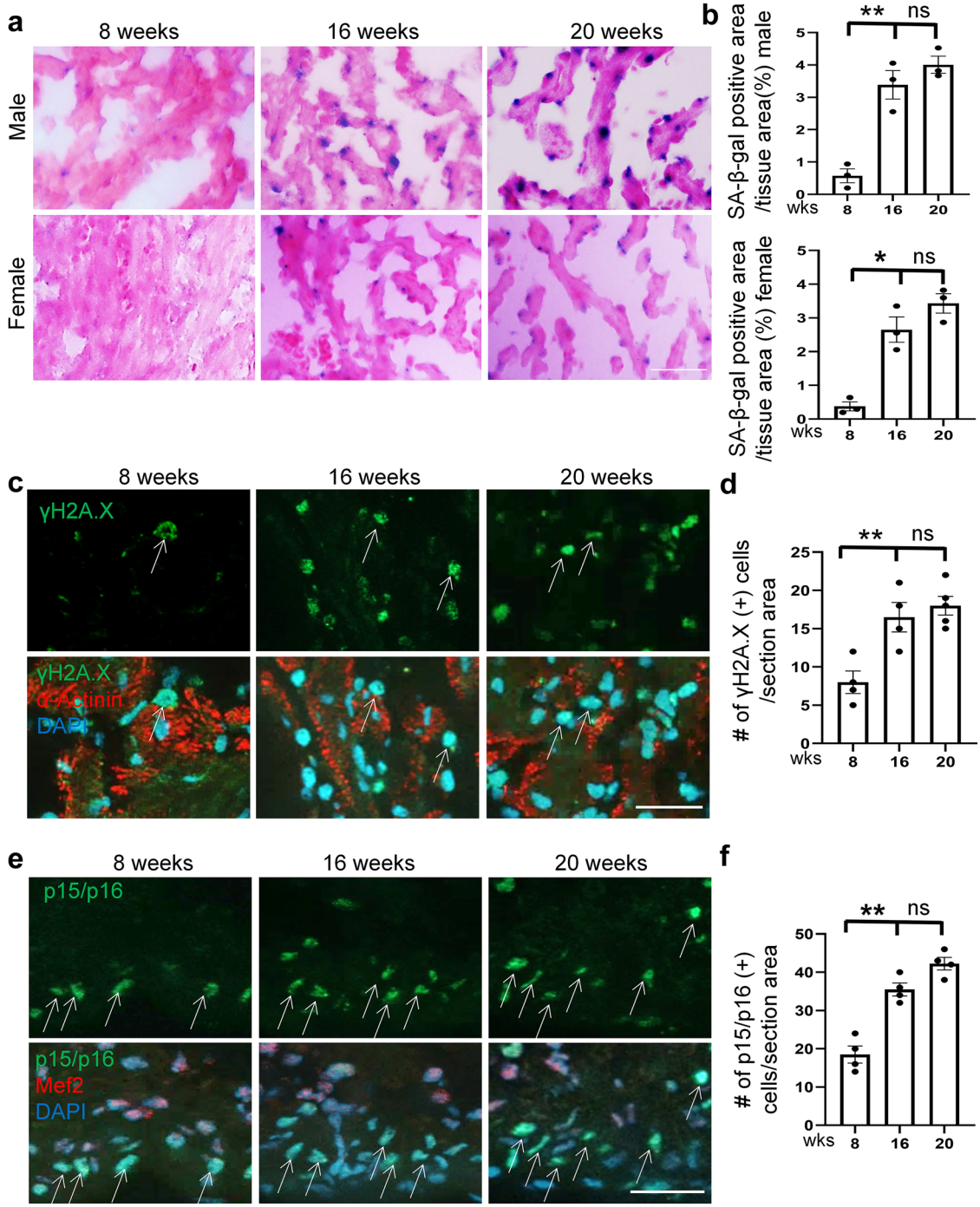

Fig. 4 | Increased cellular senescence during cardiac aging in the GRZ killifish. a, b Representative images and quantification of senescence-associated beta-galactosidase (SA-β-gal) activity in heart sections from 8 to 16 weeks of age. **c–f** Representative images and quantification of immunofluorescence staining of γ-H2A.X (a DNA damage marker) co-stained with the sarcomere marker α-Actinin and p15/p16 (a cellular senescence marker) co-stained with the cardiomyocyte nucleus marker Mef2 in heart sections. Scale bars in (**a**), 100 μm; in (**c** and **e**), 20 μm. $n = 3–4$ animals. One-way ANOVA, Tukey post hoc, $^{*}p < 0.05$, $^{**}p < 0.01$.

genetic studies. Given that a 4-week life in the GRZ strain roughly corresponds to a 10-year life in human, the killifish GRZ line is a highly efficient vertebrate model for assessing compounds with potential gerotherapeutic effects. Beyond its advantage in pharmacological studies, the extremely short lifespan of killifish could also open the door for genetic studies of cardiac aging at an unprecedented scale. For example, it would be interesting to explore whether the powerful forward genetic screening approach recently established in adult zebrafish can be extended to killifish for discovering aging-associated genes[39].

Methods

Animals

The African turquoise killifish (GRZ strain) were maintained under a 14-hour light and 10-hour dark cycle at 28.5 °C and handled with care. We used a zebrafish circulation system from Aquaneering Inc. to accommodate adult killifish. Conductivity is 650–710 micro siemens. After hatching, baby fish are fed with live brine shrimp in gradually increased water volume during the first 7 days. Fish after 8 days are put into the circulation system and fed with brine shrimp 4 times per day. Under conditions of our fish facility, male GRZ fish started to manifest their

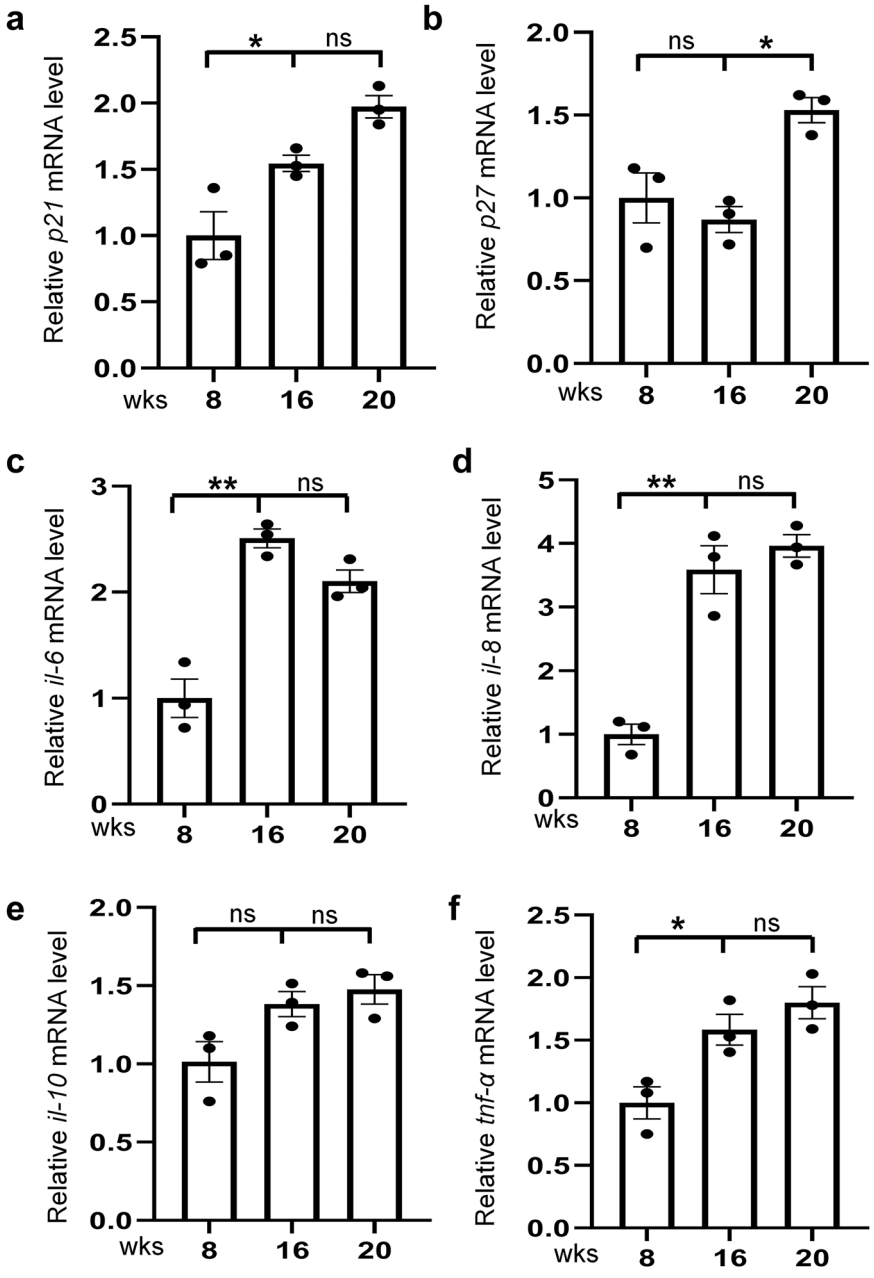

Fig. 5 | Upregulation of SASP markers during cardiac aging in the GRZ killifish. a–f Quantitative RT-PCR analysis of cell cycle arrest and SASP related markers, including *p21*, *p27*, *il-6*, *il-8*, *il-10* and *tnf-α* in heart tissues at indicated ages. $n = 3$ biological replicates. One-way ANOVA, Tukey post hoc, $^{*}p < 0.05$, $^{**}p < 0.01$.

coloration around 4–5 weeks old post-hatching. To produce eggs, 1 male and 2 female fish are accommodated in a 2.5 L tank. After fish stop to spawn, they will be fed 2 times per day. To reduce fish death because of territorial fights, we housed male fish individually in separate tanks, and females in groups of <10 fish per 2.5 L medium tank. The animal study protocol was approved by the Mayo Clinic Institutional Animal Care and Use Committee (Number: A00003390-18-R23). All animal study procedures were performed in accordance with the Guide for the Care and Use of Laboratory Animals published by the US National Institutes of Health (NIH Publication No. 85-23, revised 1996).

Body color quantification

Color quantification of killifish during physiological aging was conducted according to a previously published method with modification[40–42]. We quantified the color changes by analyzing pictures captured under controlled conditions ensuring consistent background. (Fig. S1a). The position of camera was fixed to minimize efforts of calibration[43]. Matlab was used to read the image files and to execute subsequent colorimetric analyses (Fig. S1a). The background was calibrated to ensure uniformity in color luminance reflection effect. A color atlas was applied to conform lighting environment. A surface light source was used to prevent uneven lights. Besides the RGB record method, Lightness, a-channel, b-channel (Lab) was applied to minimize the brightness difference produced by the curved body shape of fish, which helps to ensure consistent color quantification[44].

Guided by manually annotated landmarks, the fish photograph is divided into 17 distinct regions (Fig. S1b), each reflecting a specific area of interest. The segmentation is performed using the k-means color clustering method. The diagram provides only a conceptual representation of regional divisions, and the boundaries shown are approximate indications rather than precise segmentation delineations, serving as a general framework for visualization purposes. The coordinates and boundaries of these regions were determined by annotated points and physiological landmarks on the fish, respectively. For example, we use K-means clustering algorithm to separate the yellow tail region of the fish. As the yellow regions change with age, we adjust the boundaries accordingly when making divisions. The threshold prediction method defines the boundaries of the yellow region,

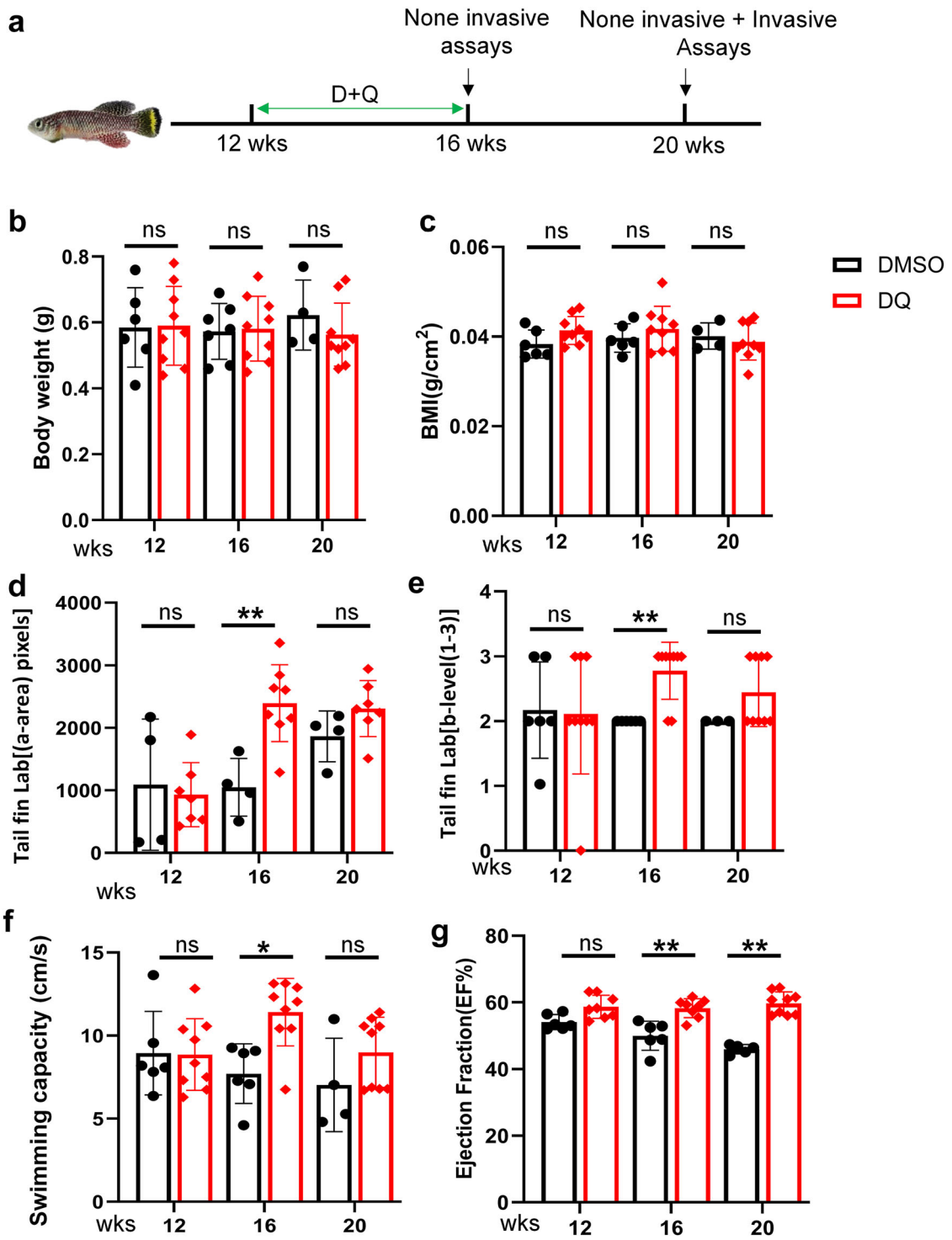

Fig. 6 | Dasatinib and Quercetin (D + Q) senolytic treatment decelerates cardiac aging in GRZ killifish. a Experimental timeline for D + Q treatment and assessments. D + Q was administered by oral gavage every other day from 12 to 16 weeks of age. Non-invasive cardiac function and swimming endurance assays were performed at 16 and 20 weeks of age, while invasive assays including SA-β-gal activity, immunofluorescence staining, and SASP quantitative RT-PCR were conducted performed at 20 weeks of age. **b, c** Body weight and BMI measurements in killifish treated with or without D + Q. **d, e** body color of the tail fin in male killifish with D + Q-treated and untreated groups at 16 and 20 weeks of age. **d** Y-axis: Tail fin Lab[(b-area) pixels], **e** Tail fin Lab[b-level(1-3)], classified yellow intensity: 1=weak, 2=moderate, 3=strong (ranges defined in Methods) (**f, g**) EF% and swimming capacity in D + Q-treated killifish compared to the DMSO control group in killifish treated with or without D + Q at 16 and 20 weeks of age. $n = 4–9$, two-way ANOVA, Tukey post hoc, $^{*}p < 0.05$, $^{**}p < 0.01$.

while K-means clustering further refines the segmentation by grouping similar colors.

RGB and Lightness, a-channel, b-channel (Lab), two color schemes developed by the International Commission on Illumination (CIE), were used to measure color values in body (sum of 17 regions in Fig. S1b), tail fin (region 4), and anal fin (region 3), respectively. RGB values (0–255) for all pixels, CIELab values. L (Lightness) scaled from 0 (black) to 100 (white); **a** (green–red axis) ranging from −128 (green) to 127 (red); **b** (blue–yellow axis) ranging from −128 (blue) to 127 (yellow). After comparing mean values and the color area distribution for

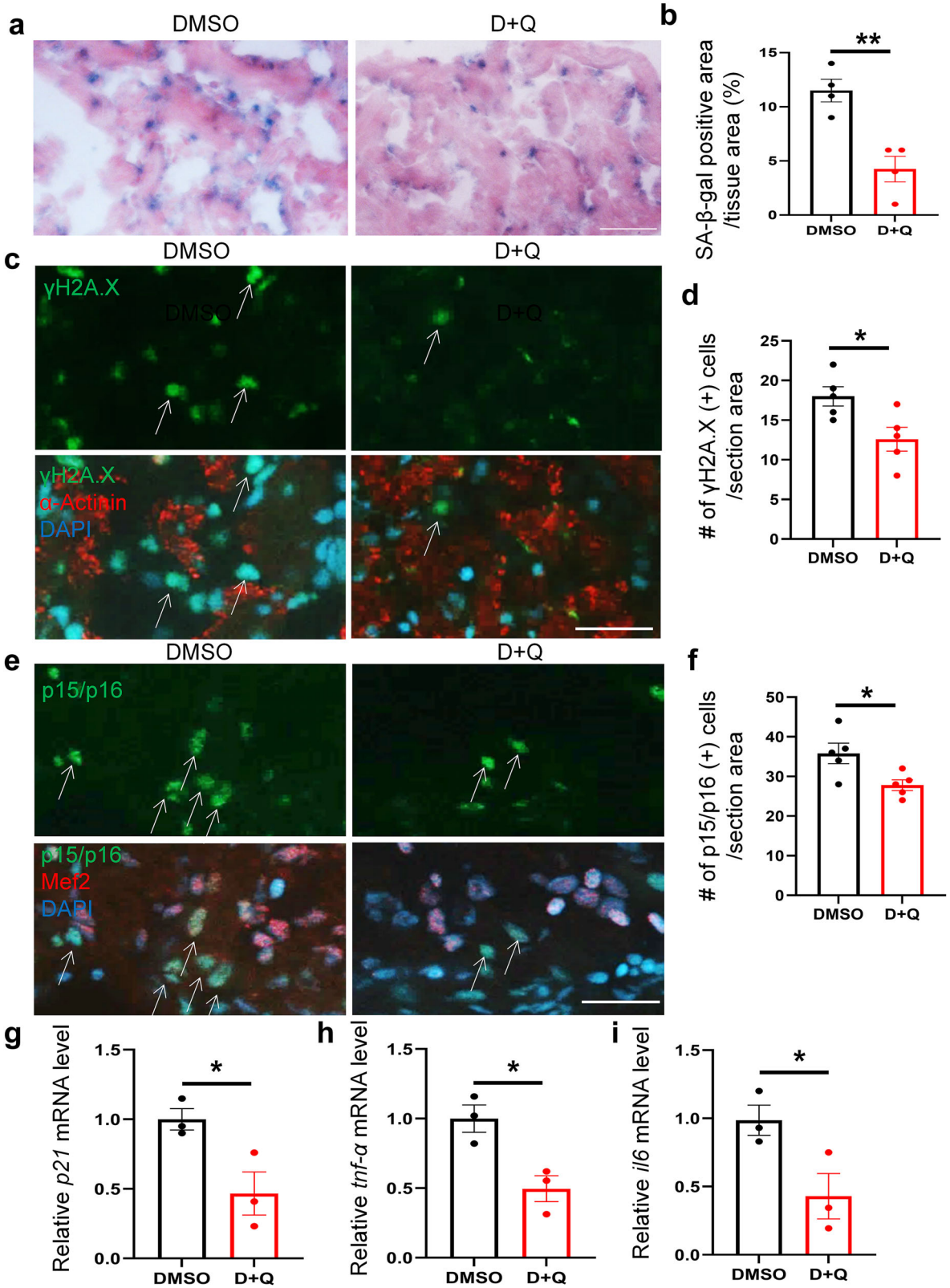

Fig. 7 | D + Q senolytic treatment removes senescent cells and inhibits SASP marker expression in GRZ killifish hearts. a, b Representative images and quantification of SA-β-gal activity staining in the D + Q treated hearts compared to DMSO controls at 20 weeks of age. Scale bar, 100 µm. $n = 3$, student's t test. **c–f** Representative images of γ-H2A.X and p15/p16 antibody immunofluorescent staining and quantification of γ-H2A.X-positive and p15/p16-positive (arrows) cell numbers in the D + Q treated killifish hearts compared to DMSO. Scale bars, 20 µm. $n = 3$, student's t test. **g–i** Quantitative RT-PCR analysis of cellular senescence marker p21 and SASP markers including *tnf-α* and *il-6* in the D + Q treated killifish hearts compared to DMSO control. $n = 3$–4 biological replicates, student's t test. $^{*}p < 0.05$, $^{**}p < 0.01$.

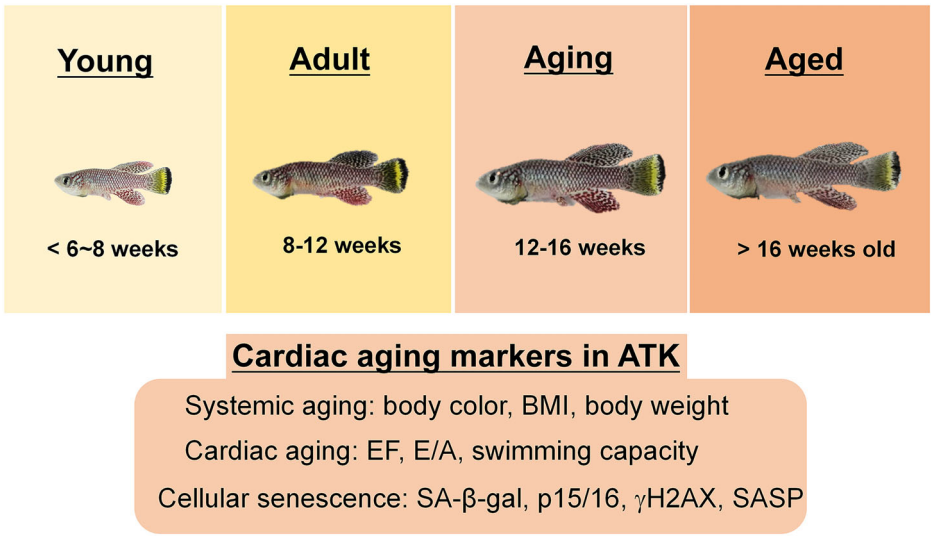

Fig. 8 | Summary of markers for quantifying cardiac aging in GRZ killifish. 8 weeks and 16 weeks have been identified as two time points along the aging process to measure cardiac aging in the GRZ killifish line. A panel of markers have been identified to quantify systemic aging, cardiac aging, and cardiac senescence processes, respectively.

different area, we chose the following parameters because of their higher sensitivity: R for whole trunk, b-area for tail fin and a-mean for anal fin.

Echocardiography

Killifish were anesthetized in 0.03% buffered tricaine (MS-222, Sigma Aldrich) for 3 min to ensure fish manifest stage III anesthesia, as indicted by loss of equilibrium and no response to tail touch. No fish die under this protocol, and 100% fish can fully recover within 1 min after dilution with fresh water. The Vevo 3100 high-frequency imaging system equipped with a 50 MHz (MX700) linear array transducer probe (FUJIFILM VisualSonics Inc) was used to measure cardiac function indices in African turquoise killifish according to a reported protocol[45]. Acoustic gel (Aquasonic® 100, Parker Laboratories, Inc) was applied to the surface of the transducer to ensure adequate coupling with the tissue interface. The MX700 probe was positioned at a slight angle above a killifish's chest to capture a two-dimensional view of the heart. The Vevo LAB 5.6.0 software was used to analyze measurements on systolic and diastolic dimensions of the ventricle, enabling calculations of ejection fraction and other ventricular function indices.

E/A ratio Measurement: The E/A ratio was measured using pulsed-wave Doppler, recording the peak early diastolic filling velocity (E-wave, cm/s) and the peak late diastolic (atrial) filling velocity (A-wave, cm/s). Left ventricular ejection fraction (EF%) was calculated from B-mode images using the formula: [(End-Diastolic Volume (EDV, μL) - End-Systolic Volume (ESV, μL)) / EDV] × 100. Both EDV and ESV were measured over 3 consecutive cardiac cycles, and the results were averaged.

Swimming tunnel assay

A swim tunnel respirometer (Mini Swim170, Loligo Systems, Danmark) was used to measure the swimming capacity of turquoise killifish. This protocol was derived from previous reports[37,46]. Briefly, turquoise killifish at designated age were fasted for 24 h before the first swimming capacity measurement. To evaluate swimming capacity, killifish were transferred, four to eight fish per group, into the swim tunnel respirometer with an initial water speed of 9 cm/s for a 20-min acclimation period. Water flow was then increased in stages of 8.66 cm/s (Ti) every 150 s (Tii) until all killifish were exhausted. The speeds at the last stage (Uii) and the previous stage (Ui) were recorded for each individual fish. The critical swimming capacity (Ucrit) was calculated with the following formula: Ucrit=Ui + [Uii×(Ti/Tii)]. Ucrit was then normalized to the body length (BL) of the corresponding individual. The swimming test was longitudinal, at 8, 12, 16 and 20 weeks of ages, respectively. For each time point, a single swimming test was performed.

Senescence-associated beta-galactosidase (SA-β-gal) staining

SA-β-gal staining was performed using the Senescence β-Galactosidase Staining Kit (Cell Signaling Technology, catalog #: 9860) according to the manufacturer's instructions, with modifications. Briefly, killifish hearts were dissected and immediately fixed overnight at 4 °C in 4% paraformaldehyde (PFA) buffered with PBS. The fixed hearts were embedded in a tissue freezing medium and sectioned at 8 μm using a cryostat (Leica CM3050 S). The heart sections were further fixed in the provided fixation solution and stained in the X-gal staining solution from the kit for 5–12 h at 37 °C. X-gal-stained sections were imaged using a Zeiss Axioplan 2 microscope (Carl Zeiss). SA-β-gal activity was quantified with MetaMorph software (64-bit) version 7.10.5.476.

Antibody immunostaining

Heart samples dissected from killifish at designated stages were embedded in a tissue freezing medium and sectioned at 8 μm using a cryostat (Leica CM3050 S). Sections were air dried for 30 min at room temperature (RT) and fixed with 4% PBS-buffered paraformaldehyde (PFA) for 7 mins, permeabilized with 0.1% Triton X-100 in PBD (1X PBS, 1% BSA, 1% DMSO) for 45 mins, blocked with 2% sheep serum/PBD for 25 mins, and incubated with primary antibodies overnight at 4°C. Primary antibody-stained sections were then washed in PBD for three times and incubated with secondary antibodies (Alexa Fluor anti-Rabbit 488, ThermoFisher Scientific, catalog #A11008; Alexa Fluor anti-Mouse 568, ThermoFisher Scientific, catalog #A11001) at RT for 1 h, washed with PBD for three times and transferred to a slide with a mounting medium with DAPI (Vector, H-1200). Stained sections were imaged with a Zeiss Axioplan 2 microscope equipped with ApoTome and AxioVision software (Carl Zeiss). The following primary antibodies were used: mouse anti-p16 (1:100, Santa Cruz, catalog #sc-1661), rabbit anti-γH2A.X (phosphor Ser139) (1:200, GeneTex, catalog #GTX127342), and mouse anti-α-actinin (1:300, Sigma, catalog #A7811).

Quantitative real-time PCR to quantify expression of SASP markers

Quantitative real-time PCR was used to quantify the expression levels of senescence-associated secretory phenotype (SASP) markers. Briefly, total RNA was extracted from an individual African turquoise killifish ventricle at designated stages using Trizol reagent (ThermoFisher Scientific) following the manufacturer's instruction. Approximately 100 ng total RNA was used for reverse transcription (RT) and cDNA synthesis using Superscript III First-Strand Synthesis System (ThermoFisher Scientific). Real-time quantitative PCR was performed in 96-well optical plates (ThermoFisher Scientific) using an Applied Biosystem VAii 7 System (ThermoFisher Scientific). Gene expression levels were normalized using the expression

level of *18 s* by −ΔΔCt (cycle threshold) values. Primer information for qRT-PCR is listed as follows:

p21-F, 5'-CGAGCCCTCAGTACTCTAA-3'
p21-R, 5'-GAGGTTTGTCGGAGAAGAAG-3'
p27-F, 5'-GCTCCTCAATCGCCATATT -3'
p27-R, 5'-CATACGTCGAAGTGGAAGAC-3'
tnf-α-F, 5'-CAGGCTCACAAGAGGTTATT-3'
tnf-α-R, 5'-CCAGAGGTCAATCTGTCTTATC-3'
il6-F, 5'-GGAGGAATTTCAAGGGAACATA-3'
il6-R, 5'-CCTCAGGAGAACCATGTAGA-3'
il8-F, 5'-ACAAATCCTGACCACAAGTAG-3'
il8-R, 5'-ATCGTATTCACCATCATGTCTC-3'
il10-F, 5'-CCTTACAGCATCATGTCTCTC-3'
il10-R, 5'-TGGCAGCAGTCGTTTATG-3'
18s-F, 5'-CCGACATTGACCTCAACAA-3'
18s-R, 5'-TGGCTGTATTTGCCATCC-3'

Dasatinib and quercetin (D + Q) administration

Dasatinib (MilliporeSigma) and Quercetin (Sigma Aldrich) administration were conducted via oral gavage every other day from 12 to 16 weeks of age, according to the previously published method. The doses are 0.5 mg/kg D and 5 mg/kg Q, which are dissolved in 1% DMSO[12]. The control group were gavaged with 1% DMSO solution.

We used the same protocol for gavaging in adult killifish, as we reported in adult Zebrafish[47]. In short, killifish were anesthetized in 0.03% buffered tricaine (MS-222, Sigma Aldrich) for 3 min. The fish mouth was opened, and a soft 187 catheter tube (Braintree Scientific) was inserted 1.0 ~ 1.5 cm deep to reach the fish stomach. In general, the insertion process was unobstructed; however, any obstructions encountered were circumvented by changing the insertion angle. The drug was released in the fish when the syringe was depressed. The delivery volume was less than 1 μl/100 mg body weight.

Data availability

All the data is derived from the self-established databases. The datasets requested and/or used during all else studies are available from the corresponding author upon reasonable request.

Received: 13 April 2025; Accepted: 25 June 2025;
Published online: 11 July 2025

References

1. Maldonado, E. et al. Aging hallmarks and the role of oxidative stress. *Antioxidants* **12**, 651 (2023).
2. Lazzeroni, D. et al. The aging heart: A molecular and clinical challenge. *Int. J. Mol. Sci.* **23**, 16033 (2022).
3. Aging Biomarker Consortium A biomarker framework for cardiac aging: The Aging Biomarker Consortium consensus statement. *Life Med.* **2**, lnad035 (2023).
4. Vetrano, D. L. et al. Fostering healthy aging: The interdependency of infections, immunity and frailty. *Ageing Res. Rev.* **69**, 101351 (2021).
5. Cameli, M. et al. Echocardiographic assessment of left ventricular systolic function: from ejection fraction to torsion. *Heart Fail Rev.* **21**, 77–94 (2016).
6. Wu, J. et al. Echocardiography E/A Abnormality is Associated with the Development of Primary Left Ventricle Remodeling in Middle-Aged and Elderly Women: A Longitudinal Study. *Clin Interv Aging* **18**, 629–638 (2023).
7. Ma, X. & Xu, X. A swimming-based assay to determine the exercise capacity of adult zebrafish cardiomyopathy models. *Bio Protoc.* **11**, e4114 (2021).
8. North, B. J. & Sinclair, D. A. The intersection between aging and cardiovascular disease. *Circ. Res.* **110**, 1097–1108 (2012).
9. López-Otín, C. et al. Hallmarks of aging: An expanding universe. *Cell* **186**, 243–278 (2023).
10. Abdellatif, M. et al. Hallmarks of cardiovascular ageing. *Nat. Rev. Cardiol.* **20**, 754–777 (2023).
11. Childs, B. G. et al. Cellular senescence in aging and age-related disease: from mechanisms to therapy. *Nat Med.* **21**, 1424–1435 (2015).
12. Van Houcke, J. et al. A short dasatinib and quercetin treatment is sufficient to reinstate potent adult neuroregenesis in the aged killifish. *NPJ Regen Med.* **8**, 31 (2023).
13. Vanhunsel, S. et al. The killifish visual system as an in vivo model to study brain aging and rejuvenation. *NPJ Aging Mech Dis.* **7**, 22 (2021).
14. Harel, I. & Brunet, A. The African turquoise killifish: A model for exploring vertebrate aging and diseases in the fast lane. *Cold Spring Harb. Symp. Quant. Biol.* **80**, 275–279 (2015).
15. Baumgart, M. et al. RNA-seq of the aging brain in the short-lived fish N. furzeri - conserved pathways and novel genes associated with neurogenesis. *Aging Cell* **13**, 965–974 (2014).
16. Hu, C. K. & Brunet, A. The African turquoise killifish: A research organism to study vertebrate aging and diapause. *Aging Cell* **17**, e12757 (2018).
17. Xu, A. et al. Transcriptomes of aging brain, heart, muscle, and spleen from female and male African turquoise killifish. *Sci Data* **10**, 695 (2023).
18. Kim, Y., Nam, H. G. & Valenzano, D. R. The short-lived African turquoise killifish: An emerging experimental model for ageing. *Dis. Model. Mech.* **9**, 115–129 (2016).
19. Schöfer, S. et al. Senescence-associated ß-galactosidase staining over the lifespan differs in a short- and a long-lived fish species. *Eur J Histochem* **68**, 3977 (2024).
20. Wendler, S. et al. Age-dependent decline in fin regenerative capacity in the short-lived fish Nothobranchius furzeri. *Aging Cell* **14**, 857–866 (2015).
21. Roos, C. M. et al. Chronic senolytic treatment alleviates established vasomotor dysfunction in aged or atherosclerotic mice. *Aging Cell* **15**, 973–977 (2016).
22. Chin, T. et al. The role of cellular senescence in skin aging and age-related skin pathologies. *Front. Physiol.* **14**, 1297637 (2023).
23. Ortonne, J. P. Pigmentary changes of the ageing skin. *Br. J. Dermatol.* **122**, 21–28 (1990).
24. Ambrosini, A. P. et al. Chronic coronary disease in older adults. *Med. Clin. North Am.* **108**, 581–594 (2024).
25. Kishi, S. Functional aging and gradual senescence in zebrafish. *Ann. N. Y. Acad. Sci.* **1019**, 521–526 (2004).
26. Khan, S. S. et al. Association of body mass index with lifetime risk of cardiovascular disease and compression of morbidity. *JAMA Cardiol.* **3**, 280–287 (2018).
27. Alley, D. E. et al. A research agenda: The changing relationship between body weight and health in aging. *J. Gerontol. A Biol. Sci. Med. Sci.* **63**, 1257–1259 (2008).
28. Forman, D. E. et al. Impact of incident heart failure on body composition over time in the Health, Aging, and Body Composition Study population. *Circ. Heart Fail.* **10**, e003915 (2017).
29. Zhang, T. Y. et al. Effect of aging and sex on cardiovascular structure and function in wild type mice assessed with echocardiography. *Sci. Rep.* **11**, 22800 (2021).
30. Abou-Dahech, M. S. & Williams, F. E. Aging, age-related diseases, and the zebrafish model. *J. Dement. Alzheimer's Dis.* **1**, 48–71 (2024).
31. Nieto, M., Konigsberg, M. & Silva-Palacios, A. Quercetin and dasatinib, two powerful senolytics in age-related cardiovascular disease. *Biogerontology* **25**, 71–82 (2024).
32. Fleg, J. L. & Strait, J. Age-associated changes in cardiovascular structure and function: A fertile milieu for future disease. *Heart Fail. Rev.* **17**, 545–554 (2012).
33. Ogawa, T. et al. Effects of aging, sex, and physical training on cardiovascular responses to exercise. *Circulation* **86**, 494–503 (1992).

34. Goldspink, D. F. Ageing and activity: Their effects on the functional reserve capacities of the heart and vascular smooth and skeletal muscles. *Ergonomics* **48**, 1334–1351 (2005).
35. Fuentes-Abolafio, I. J. et al. Physical functional performance and prognosis in patients with heart failure: A systematic review and meta-analysis. *BMC Cardiovasc. Disord.* **20**, 512 (2020).
36. Zoladz, J. A. et al. Characterization of age-dependent decline in spontaneous running performance in the heart failure Tgαq*44 mice. *J. Physiol. Pharmacol*. **72**, (2021).
37. Sun, Y. et al. Evidence of an association between age-related functional modifications and pathophysiological changes in zebrafish heart. *Gerontology* **61**, 435–447 (2015).
38. Takahashi, C. et al. Single housing of juveniles accelerates early-stage growth but extends adult lifespan in African turquoise killifish. *Aging* **16**, 12443–12472 (2024).
39. Ding, Y. et al. A modifier screen identifies DNAJB6 as a cardiomyopathy susceptibility gene. *JCI Insight* **1**, e88797 (2016).
40. Igiel, C. et al. Reliability of visual and instrumental color matching. *J. Esthet. Restor. Dent.* **29**, 303–308 (2017).
41. Illumination ICo. CIE Technical Report Colorimetry. 3rd ed. (United States: Illumination ICo, 2004).
42. Methods for the measurement of object color. GBT3979-2008, (2008).
43. Sampaio, C. S. et al. Variability of color matching with different digital photography techniques and a gray reference card. *J. Prosthet. Dent.* **121**, 333–339 (2019).
44. Boksman, L. Shade selection: Accuracy and reproducibility. *Ontario Dentist* **84**, 24 (2007).
45. Zhang, H. et al. A Langendorff-like system to quantify cardiac pump function in adult zebrafish. *Dis. Model. Mech*. **11**, (2018).
46. Taegtmeyer, H. et al. Return to the fetal gene program: a suggested metabolic link to gene expression in the heart. *Ann N Y Acad Sci.* **1188**, 191–198 (2010).
47. Wang, Y. et al. atg7-Based autophagy activation reverses doxorubicin-induced cardiotoxicity. *Circ. Res.* **129**, e166–e182 (2021).

Acknowledgements

This study was supported in part by grants from the NIH (HL107304 and HL081753), a Center for Biomedical Discovery (CBD) and Cardiovascular Research Center (CVRC) award from the Mayo Foundation, and an Award from the Mayo Clinic Robert and Arlene Kogod Center on Aging to X.X. Special thanks to Dr. Chi-Kuo HU, Stony Brook University, who shared GRZ fish embryos and provided invaluable guidance on killifish husbandry. We also thank Beninio Gore, Quentin Stevens, Briana Skufca, Rachel Helgerson, and Anastasia Noiheuan for managing the Mayo zebrafish/killifish facility.

Author contributions

Conceptualization: X.M., Y.D., D.M.R., and X.X.; Methodology: X.M., Y.D., D.M.R., X.Z., Y.L and M.M; Software: X.M., Y.D., D.M.R., X.Z., Y.L., P.Y., F.Y., and Y.L.; Validation: X.M. and Y.D.; Formal analysis: X.M., Y.D., X.Z., Y.L., D.M.R. and X.X.; Data curation: X.M., Y.D., X.Z., and Y.L.; Writing—original draft: X.M. and X.X.; Writing—review and editing: X.M., Y.D., D.M.R., and X.X.; Supervision: X.X.; Project administration: X.X.; and Funding acquisition: X.X.

Competing interests

The authors declare no competing interests.

Additional information

Supplementary information The online version contains supplementary material available at https://doi.org/10.1038/s41514-025-00253-w.

Correspondence and requests for materials should be addressed to Xiaolei Xu.